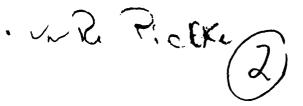
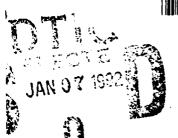
AD-A244 146





Mesoscale Vertical Velocities Generated

by

Stress Changes in the Boundary Layer: Linear Theory

G.A. Dalu, M. Baldi, R.A. Pielke, J.T. Lee, and M. Colacino,

July 15, 1991

- 1 mailing address: G.A. Dalu, Cooperative Institute for Research in the Atmosphere, CIRA-CSU, Foothill Campus, Fort Collins, CO 80523
- 2 Department of Atmospheric Science, CSU, Foothill Campus, Fort Collins, CO 80523
- 3 Institute for Atmospheric Physics, IFA-CNR, P.le L. Sturzo 31, Rome, Italy 00144
- 4 Area Ricerca Frascati, ARF-CNR, Via G. Galilei, CP 27, Frascati-Rome, Italy 00044

Abstract

We evaluate the mesoscale vertical velocity induced by stress changes in the surface layer as a function of the size of the rough patch in relation to environmental parameters. The nature of the flow perturbation strongly depends on the relation between the width of the rough patch and the two natural scales of the flow, i.e. the inverse inertia wave number and the inverse of the Scorer parameter. When the width of the rough patch is comparable to the inverse inertia wave number or larger, the atmospheric perturbation is trapped, the vertical scale equals the depth of the stress surface layer, and the horizontal scale equals the Rossby radius. When the width of the rough patch is larger than the inverse of the Scorer parameter, but smaller than the inverse inertia wave number, the atmospheric perturbation is a hydrostatic gravity wave with a vertical wave number equal to the Scorer parameter. When the width of the rough patch is comparable to the inverse of the Scorer parameter, the atmospheric perturbation is a propagating lee wave with a vertical wave number equal to the Scorer parameter. When the ambient flow is strong over a small rough patch, the flow is irrotational. The same limitations, inherent to the linear

draument has been approved this release and sale; its bution is unlimited.

91-18119

gravity waves excited by the forcing in the atmosphere (e.g. mountain waves, gravity waves initiated by convection, etc.), apply to the mesoscale perturbation induced by a rough patch.

1 Introduction

When an air mass approaches a region where there is a substantial increase of the shearing stress in the surface layer, the air speed decelerates in the lower layer. The resulting horizontal convergence is associated with rising motion. Such situations are typical, for example, in coastal urban areas when onshore flow occurs. However, it may also be of significance in inland urban areas, because of the contrast with surrounding agricultural rural areas or when there is a contrast between prairie and wooded areas. The developed vertical velocities may trigger, under supportive synoptic conditions, convective clouds. The features of the induced vertical velocity may also be of importance in dispersing pollutant.

In this paper we approach the problem of the vertical velocity which arises because of horizontal inhomogeneities in the surface shearing stress in the atmospheric planetary boundary layer. This study is an extension in more general terms of a previous paper (Dalu et al. 1988), where we report on the waves generated by a change in surface roughness (CSR).

Hunt and Simpson (1982) provide an excellent review of the studies reported by that time, concerning flow perturbations induced by a roughness change. Furthermore Hunt (Belcher et al, 1990) and at the EUROMEC 1990 meeting presented solutions concerning the flow perturbation induced by roughness changes within and around the stress layer. Our work generally agrees with his results, however it is less detailed in the structure of the perturbation within the stress layer, because we are more concerned with the flow perturbation in the free atmosphere above. Additional studies reporting on the impact of a sudden change in the surface roughness on the horizontal flow are given by Pendergrass and Arya (1984).

Claussen (1987) computed, using a model simulation, the vertical velocity due to a CSR. However, the computed vertical velocities were, in general, very sensitive to the horizontal grid resolution, which must often be reduced to several hundred meters in order to appropriately resolve the related vertical velocity. Using a very coarse horizontal resolution, Vukovich and Dunn (1978) in their numerical model simulation of the St. Louis urban area, suggested that the surface rough-

ness has only a small effect on the circulation for the wind speeds used in their study. Alestalo et al. (1985), using a hydrostatic two-dimensional model with a grid interval of 4 km simulated the airflow in the Baltic shore region of Finland, and found a maximum for the vertical velocity of order of 1 cm s^{-1} , due to the CSR. They attributed the reported increase of precipitation in that area, in the absence of thermal forcing, to the vertical velocity induced by the CSR. Pielke (1974) evaluated the magnitude of vertical velocity caused by a CSR over Florida using a 11 km horizontal resolution model. Although the magnitudes were small ($\approx 0.1 \ cm \ s^{-1}$), it was concluded t: at shallow warm-rain clouds over the southeast coast of Florida could result due to this mechanism. Finally, Roeloffzen et al. (1986) presented a steady state model calculation of secondary flow patterns forced by a CSR. Adopting a neutral boundary layer and using a refined grid resolution. they suggest that frictional effects involved with a CSR at a coast line, can lead to a secondary circulation on the mesoscale. They suggest that this forcing is a factor in the observed coastal frontogenesis active in the early fall along the coast of the Netherlands.

2 The Governing Equation for the Linear Problem

If we assume that the process is stationary, two-dimensional and Boussinesq, then the primitive equations in linear form can be reduced to a Scorer type equation for the vertical velocity in non-homogeneous form:

$$\left(\frac{k^2 - k_0^2}{k^2}\right)\hat{w}_{zz} + (l^2 - k^2)\hat{w} = -\frac{\hat{\tau}_{zz}}{\rho U}$$
 (1)

Because of the linearization the perturbations may be underestimated, however, since the solutions are continuous, there are no limitations due to grid-size. For a derivation of equation (1), see Eliassen (1977). The hat denotes the Fourier transform of the variable, k is the horizontal wave number, $k_0 = f/U$ is the inertial wave number (f is the Coriolis parameter, U is the ambient flow perpendicular to the change in surface roughness, and U_z is its shear), τ is the resulting shear stress, and l is the Scorer parameter:

$$l^2 = \frac{N^2}{U^2} - \frac{U_{zz}}{U} \quad \text{with} \quad N^2 = \frac{\partial \bar{b}}{\partial z}$$
 (2)

3

Statement A per telecon Dr. Robert Abbey ONR/Code 1122 Arlington, VA 22217-5000

where N is the Brunt-Väisäla frequency and \bar{b} is the buoyancy of the environment. Equation (1) can rewritten as:

$$\hat{w}_{zz} + \nu^2(k)\hat{w} = G^2(k)\frac{\hat{\tau}_{zz}}{\rho U}$$
 (3)

with
$$\nu^2(k) = k^2 \frac{l^2 - k^2}{k^2 - k_0^2}$$
 and $G^2(k) = \frac{k^2}{k^2 - k_0^2}$

In the wave number region where $\nu^2(k) < 0$, the waves are trapped around the perturbing source within an e-folding vertical distance equal to μ_0^{-1} . The vertical wave number μ_0 for the trapped waves is:

$$\mu_0(k) = |i \nu(k)| = |k| \sqrt{\frac{l^2 - k^2}{k_0^2 - k^2}} \quad \text{when} \quad 0 < |k| < k_0 \quad \text{or when} \quad l < |k| < \infty$$
 (4)

In the wave number region where $\nu^2(k) > 0$, the waves propagate away from the perturbing source with a vertical wave number equal to μ_1 . The vertical wave number μ_1 for the propagating waves is:

$$\mu_1(k) = \nu(k) = k \sqrt{\frac{l^2 - k^2}{k^2 - k_0^2}} \quad \text{when} \quad k_0 < |k| < l.$$
 (5)

Note The theory of the mesoscale vertical velocity induced by a rough patch is formulated within the framework of the well established gravity wave theory, therefore solutions in the presence of variable Scorer parameter, shear in the ambient flow, regions of neutral stability, and critical levels can be easily treated, because the related mathematical tools are already in the literature.

2.1 Green Functions and Boundary Condition

The advantage of writing the solution in terms of Green functions is that a variety of different vertical profiles of the stress could be easily studied through a simple convolution integral. Using Green function theory (Stakgold, 1979), we seek for the solutions, $\hat{g}(k, z - z')$, associated with the governing equation (1) for a point source forcing $\delta(x', z')$, which satisfies the boundary condition:

$$\hat{g}(k, z - z') = 0 \quad \text{when} \quad z = 0 \tag{6}$$

Then the vertical velocity for a given forcing is:

$$\hat{w}(k,z) = \int_0^z dz' \, \hat{g}(k,z-z') \frac{G^2(k)\hat{\tau}_{zz}(k,z')}{\rho U} \quad \Rightarrow \quad w(x,z) = \frac{1}{2\pi} \int_{-\infty}^{\infty} dk \, \hat{w}(k,z) \, \exp ixk \tag{7}$$

The Green function for the upward propagating wave, which satisfies the radiation condition (Sommerfeld, 1912 and 1948) and the boundary condition, is:

$$\hat{g}_1(k, z - z') = \frac{1}{2i\mu_1(k)} \left[\exp i(kx + \mu_1(k) |z - z'|) - \exp i(kx + \mu_1(k) |z + z'|) \right]$$
 (8)

The second term is the mode reflected by the ground.

Remark For verification, we derive the boundary value Green function, $\hat{g}_{BC}(k,z)$:

$$\hat{g}_{BC}(k,z) = -\lim_{z' \to 0} \left[\frac{\partial}{\partial z'} \hat{g}_{up}(k,z-z') \right]_{z'=0} = \exp i(kx + \mu_1(k)z)$$
 (9)

which is the Green function for a radiative wave in the mountain wave problem (Smith, 1979).

$$\hat{g}_0(k, z - z') = -\frac{1}{2\mu_0(k)} \left[\exp(ikx - \mu_0(k)|z - z'|) - \exp(ikx - \mu_0(k)|z + z'|) \right]$$
 (10)

The second term is the mode reflected by the ground.

The Green function for the upward trapped wave is:

Remark For verification, we derive the boundary value Green function, $\hat{g}_{BC}(k,z)$:

$$\hat{g}_{BC}(k,z) = -\lim_{z' \to 0} \left[\frac{\partial}{\partial z'} \hat{g}_{up}(k,z-z') \right]_{z'=0} = \exp(ikx - \mu_0(k)z)$$
(11)

which is the Green function for the trapped wave in the mountain problem (Smith. 1979).

3 Atmospheric Response to Stress Changes in the Surface Layer

The stress has the same direction and opposes the ambient flow; furthermore, for simplicity, we assume that the stress decays linearly with altitude within the stress layer:

$$\tau(x,z) = \tau_0 \ He(h-z) \frac{h-z}{h} F(x) \tag{12}$$

where τ_0 is the surface shear stress, F(x) is its horizontal distribution, and $H\epsilon$ is the Heaviside function. The mesoscale perturbation depends mainly on the intensity of the stress and on its depth, and weakly on its vertical distribution. The relation between the surface stress τ_0 , the wind intensity U, the surface drag C_D , and the shear velocity u^* is given by (Panofsky and Dutton, 1984):

$$C_D = \frac{u^{*^2}}{U^2} = \frac{\tau_0}{\rho U^2} = O\left(\frac{\kappa^2}{(\ln z/z_0)^2}\right)$$
 (13)

Here u^* is the shear velocity, κ is the von Karman constant and z_0 is the surface roughness. The atmospheric response, to a horizontal distribution of the stress (F(x)) is assumed to be an even function), is given by:

$$w(x,z) = I_{0_1} + I_1 + I_{0_2} = -\bar{w}\frac{2}{\pi} \left\{ \int_0^{k_0} dk \ G_0(k) w_{\mu_0}(k,z) \tilde{F}(k) + \int_{k_0}^l dk \ G_1(k) w_{\mu_1}(k,z) \tilde{F}(k) \right\}$$

$$+ \int_{l}^{\infty} dk \ G_0(k) w_{\mu_0}(k, z) \tilde{F}(k) \right\} \quad \text{with} \quad \bar{w} = \frac{\tau_0}{\rho U} \frac{1}{lh} = \frac{u^{*2}}{U} \frac{1}{lh} = \frac{C_D U^{*2}}{hN}$$
 (14)

The variable \bar{w} is the amplitude of the perturbation of the vertical velocity. Here

$$G_0(k) = -\frac{lG^2(k)}{\mu_0(k)} = \frac{lk}{\sqrt{(k_0^2 - k^2)(l^2 - k^2)}} \quad \text{and} \quad G_1(k) = \frac{lG^2(k)}{\mu_1(k)} = \frac{lk}{\sqrt{(k^2 - k_0^2)(l^2 - k^2)}}$$
(15)

The $w_{\mu_0}(k,z)$ waves are trapped around the top of the stress layer:

$$w_{\mu_0}(k,z) = \frac{1}{2} \left\{ \exp(-\mu_0|z-h|) - \exp(-\mu_0|z+h|) \right\} \cos(kz)$$
 (16)

The $w_{\mu_1}(k,z)$ waves propagate away from the top of the stress layer:

$$w_{\mu_1}(k,z) = \frac{1}{2} \left\{ \sin(\mu_1|z-h|+kx) - \sin(\mu_1|z+h|+kx) \right\}$$
 (17)

The tilde denotes the cosine Fourier transform:

$$\tilde{F}(k) = \int_0^\infty dx \ F(x) \cos(kx) \quad \Rightarrow \quad F(x) = \frac{2}{\pi} \int_0^\infty dk \ \tilde{F}(k) \cos(kx)$$

4 Vertical Velocity Excited by a Bell Shaped Stress

We assume that the drag coefficient is $C_D = 3 \cdot 10^{-3}$, that the depth of the stress layer is h = 300 m. and that the environment parameters have the following values $N = 10^{-2}$ s⁻¹ and $f = 10^{-4}$ s⁻¹. We evaluate the vertical velocity induced by a rough patch with a horizontal extension a, in relation to the ambient wave numbers k_0 and l. A bell shape distribution of the stress is ideal for this kind of analysis (as shown by Queney (1947) and by Smith (1979) for the vertical velocity induced by a bell shape mountain):

$$\tau_{zz}(x,z) = \frac{\tau_0 \delta(z-h)}{h^2} \frac{a^2}{a^2 + x^2} \quad \Rightarrow \quad \tilde{\tau}_{zz}(k,z) = \frac{\tau_0 \delta(z-h)}{h^2} \frac{\pi}{2} \exp(-ak); \tag{18}$$

Here δ is the Dirac function. From eq. (14) the vertical velocity is given by:

$$w(x,z) = I_{0_1} + I_1 + I_{0_2} = -\bar{w} \left\{ \int_0^{k_0} dk \ G_0(k) w_{\mu_0}(k,z) \ a \ \exp(-ak) + \int_{k_0}^l dk \ G_1(k) w_{\mu_1}(k,z) \ a \ \exp(-ak) + \int_l^{\infty} dk \ G_0(k) w_{\mu_0}(k,z) \ a \ \exp(-ak) \right\}$$
(19)

(a) - When $la >> k_0a >> 1$, $I_{0_1} >> I_1 + I_{0_2}$; the perturbation is horizontally and vertically trapped inertia wave.

Due to the exponential decay of the Fourier transform of the bell function for increasing values of the wave number, when the rough patch is large and the ambient flow is very weak, the contributions of the second and third integrals are negligible in comparison to the contribution of the first integral:

$$w(x,z) \approx I_{0_1} = \bar{w} \frac{a}{2k_0} \int_0^\infty dk \ k \left[\exp{-k \left(a + \frac{N}{f} |z + h| \right)} - \exp{-k \left(a + \frac{N}{f} |z - h| \right)} \right] \cos(kx)$$

$$= \bar{w} \frac{a}{2k_0} \left\{ \frac{\left(a + \frac{N}{f} |z + h| \right)^2 - x^2}{\left[\left(a + \frac{N}{f} |z + h| \right)^2 + x^2 \right]^2} - \frac{\left(a + \frac{N}{f} |z - h| \right)^2 - x^2}{\left[\left(a + \frac{N}{f} |z - h| \right)^2 + x^2 \right]^2} \right\}$$
(20)

This solution represents an inertia wave which is horizontally and vertically trapped, as shown in Fig.1a. When the inertial wave number is large (in Fig.1a $k_0a = 3$ and a = 100km) the air particles are displaced upward and northward within a Rossby radius distance upstream of the rough patch, then the restoring Coriolis force brings them back to the previous location through an inertial oscillation. The maximum intensity of the perturbation occurs at z = h, and monotonically decreases above it as in the Ekman solution.

(b) - When $la^2 >> k_0 a = O(1)$, $I_{0_1} >> I_1 + I_{0_2}$; the perturbation is vertically trapped inertia wave.

In this case, the second integral does not contribute significantly because of rapid oscillations of the sine argument; the third integral does not contribute because of the exponential decay, thus

$$w(x,z) \approx I_{0_1} = \bar{w} \frac{a}{2} \int_0^{k_0} dk \, \frac{k}{\sqrt{k_0^2 - k^2}} \left[\exp{-k \left(a + \frac{l |z + h|}{\sqrt{k_0^2 - k^2}} \right)} - \exp{-k \left(a + \frac{l |z - h|}{\sqrt{k_0^2 - k^2}} \right)} \right] \cos(kx) (21)$$

This solution represents a number of vertically trapped inertial oscillations (Fig.1b). Again, the perturbation monotonical decays with altitude above the stress layer.

(c) - When $la >> 1 >> k_0a$, $I_1 >> I_{0_1} + I_{0_2}$; the perturbation is a hydrostatic gravity wave.

In this case, the trapped wave contribution is negligible in comparison to the contribution of a vertically propagating hydrostatic wave:

$$w(x,z) \approx I_1 = \bar{w} \frac{a}{2} \int_0^\infty dk \left[\sin(l|z+h|+kx) - \sin(l|z-h|+kx) \right] \exp(-ak)$$

$$= \frac{\bar{w}}{2} \frac{a}{[a^2 + x^2]} \left\{ \left[a \sin(l|z+h|) + x \cos(l|z+h|) \right] - \left[a \sin(l|z-h|) + x \cos(l|z-h|) \right] \right\}$$
(22)

The hydrostatic gravity wave is shown in Fig.2a. When the inverse of the Scorer parameter is smaller than the extension of the rough patch (la = 3 and a = 1 km in Fig.2a), the perturbation has a wave structure with a vertical wave number equal to l. The maximum intensity of the perturbation occurs at the center of the rough patch at z = h.

(d) - When $la = O(1) >> k_0 a$, $I_1 + I_{0_2} > I_{0_1}$; the perturbation is a non-hydrostatic lee wave.

For this situation, the contribution of the first integral I_{0_1} is negligible, the vertical velocity is:

$$w(x,z) \approx I_1 + I_{0_2} \tag{23}$$

However, most of the contribution is in the propagating non-hydrostatic wave:

$$I_{1} = \bar{w} \frac{a}{2} \int_{0}^{l} dk \frac{l \left[\sin(\sqrt{l^{2} - k^{2}}|z + h| + kx) - \sin(\sqrt{l^{2} - k^{2}}|z - h| + kx) \right]}{\sqrt{l^{2} - k^{2}}} \exp(-ak)$$

$$\approx \bar{w} \frac{\pi la}{4} \exp(-la) \left\{ \left[\sin(l|z + h|) J_{0}(l(x - |z + h|)) + \cos(l|z + h|) H_{0}(l(x - |z + h|)) \right] - \left[\sin(l|z - h|) J_{0}(l(x - |z - h|)) + \cos(l|z - h|) H_{0}(l(x - |z - h|)) \right] \right\}$$

The contribution of the trapped non-hydrostatic wave is:

$$I_{0_2} = \bar{w} \frac{a}{2} \int_{l}^{\infty} dk \, \frac{l \left[\exp{-(\sqrt{k^2 - l^2}|z + h|) - \exp{-(\sqrt{k^2 - l^2}|z - h|)}} \right]}{\sqrt{k^2 - l^2}} \exp(-ak) \, \cos(kx)$$

$$\approx -\bar{w} \frac{\pi \ la}{4} \exp(-la) \ N_0(lx) \left\{ \exp(-l|z+h|) - \exp(-l|z-h|) \right\}$$
 when $|lx| >> 1$

The trapped wave decays exponentially with the distance from the top of the stress layer, therefore it interferes with the propagating wave only at $z \approx h$, while weakening the propagating wave upstream and strengthening the propagating wave downstream [the zero order Neumann function is even, while the zero order Struve function is odd, with the same asymptotic behavior (Abramowitz and Stegun, 1972)], thereby producing a wake of secondary cells downstream at the level of the top of the stress layer. The non-hydrostatic lee wave is shown in Fig.2b, for la = 1 and a = 1 km). The maximum intensity of the perturbation occurs at the center of the rough patch at z = h.

(e) - When $k_0a << la << 1$, $I_{0_2} >> I_{0_1} + I_1$, and the flow is irrotational

When ambient flow is strong, the inertia wave number k_0 and the Scorer parameter l are small. Thus the contribution of the first and the second integrals are negligible, only the third integral contributes:

$$w(x,z) = I_{0z} = \bar{w} \frac{a}{2} \int_0^\infty dk \left[\exp(-(a+|z+h|)k) - \exp(-(a+|z-h|)k) \right] \cos(kx)$$

$$= \bar{w} \frac{a}{2} \left\{ \frac{(a+|z+h|)}{[(a+|z+h|)^2 + x^2]} - \frac{(a+|z-h|)}{[(a+|z-h|)^2 + x^2]} \right\}$$
(24)

The perturbation is horizontally and vertically trapped, as shown in Fig.2c for la = 0.3 and a = 1 km. The maximum intensity of the perturbation occurs at the center of the rough patch at z = h.

5 Conclusions

We have shown that a horizontal change in surface roughness can induce substantial vertical velocity. The vertical velocity can be in the form of propagating waves or in the form of trapped waves: in both cases the perturbation can be physically relevant, since the maximum is placed at the top of the stress layer, i.e. in the region where it is important to have positive vertical velocities in order to trigger cumulus convection.

The nature of this perturbations depends on the width of the rough patch relative to natural scales associated with the magnitude of inertia wave number and Scorer parameter. The vertical

scale is related to the ambient Scorer parameter, when there is vertical propagation. The horizontal scale is related to the Rossby radius for weak ambient flow over larger rough patches. When the rough patch is small, the horizontal scale is related to the inverse of the Scorer parameter.

The theory which we use is derived from mountain wave theory, (Queney, 1947; Eliassen, 1977; Smith, 1979).

Acknowledgements: This research was made possible by a grant from the National Science Fundation (ATM-89-15265) and from the Office of Naval Research (ONR) under contract (N00014-88-K-0029). G.A. Dalu, M. Baldi and M. Colacino acknowledge the support of the ENEL-CNR project (Rome - Italy) and of the Italian project Clima Territorio & Ambiente nel Mezzogiorno.

References

- Alestalo M. and H. Savijarvi, Mesoscale circulation in hydrostatic model: coastal convergence and orographic lifting. *Tellus*, 37 A, 156-162, 1985.
- Abramoviz M., Stegun I.A., Handbook of Mathematical Functions. Dover Publications, Inc., New York, 1972.
- Belcher S.E., D.P. Xu, and J.C.R. Hunt, The response of turbulent boundary layer to arbitrarily distributed two-dimensional roughness changes. Q. J. R. Met. Soc., 116, 611-635, 1990.
- Claussen M., The flow in a turbulent layer upstream of a change in surface roughness. Bound. Layer Met., 40, 31-86, 1987.
- Dalu G.A., M. Segal, T.J. Lee and R.A. Pielke. Atmospheric waves induced by change in surface roughness. *Computer Techniques in Environmental Studies*, 551-570. Editor P. Zanetti, Springer-Verlag, 1988.
- Eliassen A., Orographic waves and wave drag: Parameterization of physical effects in the atmosphere. ECMWF Seminars, 67-90, 1977.
- Garstang M., S. Ulanski, S. Greco, J. Scala, R. Swap, D. Fitzjarrald, D. Martin, E. Browell, M. Shipman, V. Connors, R. Harriss and R. Talbot, Amazon Boundary Layer Experiment (ABLE 2B): A meteorological perspective. Bull. Am. Met. Soc., 71, 19-32, 1990.
- Hunt J.C.R. and J.E. Simpson, Atmospheric boundary layer over non-homogeneous terrain.
 Engineering Meteorology, E.J. Plate Editor Elsevier, 269-318, 1982.

Panofsky H.A. and J.A. Dutton. Atmospheric turbulence. Editor John Wiley & Sons. New York, 1984.

Pendergrass W. and S.P.S. Arya, Dispersion in neutral boundary layer over a step change in surface roughness. Mean flow and turbulence structure. Atm. Env., 7, 1267-1279, 1984.

Pielke R.A., Three-dimensional numerical model of sea breeze over south Florida. Ph.D. thesis, Pen. State University, 1974.

Quency P., Theory of perturbations in stratified currents with application to airflow over mountain barriers. The University of Chicago Press, Mis. Rep. 23, 1947.

Roeleffzen J.C., W,D. Van Den Berg and J.Oerlemans, Frictional convergence at coastlines. em Tellus, 38 A, 397-411, 1986.

Smith B.R., The influence of mountains on the atmosphere. Advances in Geophysics, Academic Press, 21, 87-230, 1979.

Sommerfeld A., Die greensche funktion der schwingungsgleichung. Jahresber. Dt. Math. Ver., 21, 1912.

Sommerfeld A., Vorlesungen über theoretische physik. Akademiske Verlagsgesellschaft, Leipzig 6. Zweite neubearbeitete Auflage, pg. 191, 1948.

Stakgold I., Green's Functions and Boundary Value Problems. Editor John Wiley & Sons. New York, 1979.

Vukovich F.M. and J.W. Dunn. A theoretical study of the St. Louis heath island effect: Some parameters variations. J. Appl. Mct., 17, 1585-1594, 1978.

List of Figures

Figure 1a - Contours of vertical velocity induced by a bell shaped distributed surface stress, when the inverse of the inertial wave number is smaller than the width of the rough patch; $k_0a=3$, a=100 km, under weak flow condition (U=3 m/s, $\bar{w}=1$ cm/s and $\Delta\bar{w}=0.1$ cm/s). Figure 1b - When the ambient flow is U=10 m/s, then $k_0a=1$, $\bar{w}=10$ cm/s. and $\Delta\bar{w}=1$ cm/s. Dashed lines represent negative contour lines.

Figure 2a - Vertical velocity isolines when the inverse of the Scorer parameter is smaller than the width of the rough patch, la=3, a=1 km, under weak flow condition (U=3 m/s, $\bar{w}=1$ cm/s and $\Delta \bar{w}=0.1$ cm/s). Figure 2b - When the ambient flow is U=10 m/s, then la=1, $\bar{w}=10$ cm/s and $\Delta \bar{w}=1$ cm/s. Figure 2c - When the ambient flow is strong (U=30 m/s), then la=0.3. $\bar{w}=100$ cm/s and $\Delta \bar{w}=10$ cm/s.

Dashed lines represent negative contour lines.

